

Comparison of Uncultured Marrow Mononuclear Cells and Culture-Expanded Mesenchymal Stem Cells in 3D Collagen-Chitosan Microbeads for Orthopedic Tissue Engineering

Joel K. Wise, PhD,¹ Andrea I. Alford, PhD,² Steven A. Goldstein, PhD,^{1,2} and Jan P. Stegemann, PhD¹

Stem cell-based therapies have shown promise in enhancing repair of bone and cartilage. Marrow-derived mesenchymal stem cells (MSC) are typically expanded *in vitro* to increase cell number, but this process is lengthy, costly, and there is a risk of contamination and altered cellular properties. Potential advantages of using fresh uncultured bone marrow mononuclear cells (BMMC) include heterotypic cell and paracrine interactions between MSC and other marrow-derived cells including hematopoietic, endothelial, and other progenitor cells. In the present study, we compared the osteogenic and chondrogenic potential of freshly isolated BMMC to that of cultured-expanded MSC, when encapsulated in three-dimensional (3D) collagen-chitosan microbeads. The effect of low and high oxygen tension on cell function and differentiation into orthopedic lineages was also examined. Freshly isolated rat BMMC (25×10^6 cells/mL, containing an estimated 5×10^4 MSC/mL) or purified and culture-expanded rat bone marrow-derived MSC (2×10^5 cells/mL) were added to a 65–35 wt% collagen-chitosan hydrogel mixture and fabricated into 3D microbeads by emulsification and thermal gelation. Microbeads were cultured in control MSC growth media in either 20% O₂ (normoxia) or 5% O₂ (hypoxia) for an initial 3 days, and then in control, osteogenic, or chondrogenic media for an additional 21 days. Microbead preparations were evaluated for viability, total DNA content, calcium deposition, and osteocalcin and sulfated glycosaminoglycan expression, and they were examined histologically. Hypoxia enhanced initial progenitor cell survival in fresh BMMC-microbeads, but it did not enhance osteogenic potential. Fresh uncultured BMMC-microbeads showed a similar degree of osteogenesis as culture-expanded MSC-microbeads, even though they initially contained only 1/10th the number of MSC. Chondrogenic differentiation was not strongly supported in any of the microbead formulations. This study demonstrates the microbead-based approach to culturing and delivering cells for tissue regeneration, and suggests that fresh BMMC may be an alternative to using culture-expanded MSC for bone tissue engineering.

Introduction

REPAIR AND HEALING of critical-sized bone and severe articular cartilage defects is a major clinical challenge in orthopedics. Current clinical therapies for bone and cartilage regeneration are hampered by limited availability of autograft tissue and inconsistent effectiveness of allogeneic and biomaterial-based approaches. Stem cell-based therapies have shown promise in enhancing bone and cartilage repair. Marrow-derived mesenchymal stem cells (MSC) have shown promise in these applications and are of particular interest due to their ability to self-renew and demonstrated multipotency.^{1–6} In addition, it has been suggested that MSC exert important trophic effects,⁷ and immunomodulatory properties^{8,9} that make them attractive for cellular therapies.

Culture-expanded MSC are typically used in stem cell-based therapy due to the now well-established culture methods that allow plastic-adherent MSC to be easily manipulated and expanded to produce large quantities for proposed clinical applications. However, major disadvantages of *in vitro* culture expansion of MSC include the lengthy time and large cost, and risk of contamination. Further, two-dimensional (2D) culture-expanded MSC *in vitro* have been shown to exhibit altered antigenic and gene expression,^{10–14} loss of expression of cell surface adhesion-related chemokine receptors (CXCR4) that are imperative for homing and engraftment *in vivo*,^{15–19} and loss of multipotential differentiation capacity,^{20–22} compared with fresh uncultured MSC. Potential advantages of using fresh uncultured bone marrow progenitor cells in tissue

Departments of ¹Biomedical Engineering and ²Orthopedic Surgery, University of Michigan, Ann Arbor, Michigan.

engineered constructs include the maintenance of heterotypic cell and paracrine interactions between MSC and other marrow-derived cells, including hematopoietic stem cells (HSC), hematopoietic progenitor cells (HPC), and endothelial progenitor cells (EPC).^{23–26} In addition, unpurified marrow fractions may contain osteogenic proteins that can be incorporated into biomaterials and scaffolds.²⁷

Several previous studies have investigated direct seeding of freshly isolated uncultured bone marrow cells into three-dimensional (3D) biomaterials for bone and cartilage tissue engineering. In an ectopic implantation model in mice, direct seeding and expansion of uncultured human²⁸ or sheep²⁹ bone marrow mononuclear cells (BMMC) into 3D hydroxyapatite-ceramic scaffolds under perfusion resulted in engineered constructs that formed significantly more bone tissue than scaffolds loaded with 2D culture-expanded bone marrow-derived MSC. Additionally, it was found that the osteogenic capacity of engineered bone implants was linked to the property of clonogenicity of expanded MSC originating from directly seeded bone marrow aspirate cells.³⁰ In a critical-sized cranial defect in the rat, porous poly(L-lactic acid) scaffolds laden with uncultured BMMC encapsulated within fibrin gel regenerated significantly greater bone volume than cell-free controls.²⁷ Other recent studies have shown that 3D ceramic scaffolds directly seeded with autologous sheep bone marrow cells/MS¹² or unprocessed human bone marrow³¹ resulted in similar osteogenic potential and comparable bone formation in subcutaneous ectopic implantation models, compared with the same scaffolds seeded with culture-expanded MSC. In contrast to these reports, it has been reported that *in vitro* culture-induced osteogenic differentiation of purified human bone marrow-derived MSC seeded onto β -tricalcium phosphate ceramics significantly enhanced subsequent ectopic bone formation, compared with samples implanted with culture-expanded but undifferentiated MSC or directly seeded fresh uncultured BMMC,³² however, the authors of this study state that only 27% of the BMMCs were able to initially adhere to the particular type of scaffolds used. Another study showed that transplantation of autologous uncultured BMMC, and possibly uncultured peripheral blood-derived mononuclear cells, within fibrin gels contributed to the repair of large full-thickness articular cartilage defects.³³ Additionally, it was recently reported that uncultured BMMC contribute to the repair of full-thickness chondral defects with collagen Type II hydrogel as scaffolds, which had comparable results with culture-expanded bone marrow-derived MSCs.³⁴

Our group has used 3D hydrogel microbeads to encapsulate MSC and other progenitor cells for orthopedic tissue engineering applications. Three-dimensional microbeads of a defined size and composition, specifically consisting of a collagen-based matrix, can provide a protective and instructive microenvironment that mimics physiological aspects of *in vivo* conditions. The 3D microbead matrix surrounding the cells contributes to cell viability maintenance, and the composition of the matrix can be tailored to promote cell adhesion, proliferation, and/or desired differentiation.^{35–37} A main advantage of the microbead format is that cells (either freshly isolated or culture-expanded) can be directly embedded in microbeads, and they can then be cultured in suspension in the desired medium type until needed for delivery. Importantly, the microbeads can then be

collected without trypsinization of the cells, and can be injected as a paste in a minimally invasive manner.^{38,39} Our group has previously shown that collagen and chitosan composite hydrogels fabricated by thermal gelation and initiation using β -glycerophosphate have strong potential as matrices for cell encapsulation and scaffolds for bone tissue engineering,⁴⁰ and that cross-linking with glyoxal can be used to reinforce the mechanical properties of the gel, while maintaining cytocompatibility.⁴¹ Other investigators have also investigated the use of MSC encapsulated within collagen-based microspheres⁴² for bone,⁴³ cartilage,^{44,45} and osteochondral⁴⁶ tissue engineering.

Bone marrow, one of the main reservoirs of MSC, is estimated to have *in vivo* oxygen tension in the range of 4%–7%, much lower than the atmospheric oxygen tension (20%) used for standard cell culture.^{47–49} It has been reported that rat bone marrow-derived MSC exhibited a significantly increased number of colony-forming unit-fibroblasts (CFU-F) at primary culture, and a 40% higher cell number at first passage under hypoxia (5% O₂) compared with normoxia.^{47,48} In another study, human MSC cultured in normoxia for 30 days exhibited a decrease in CFU-F number, compared with a significant increase in CFU-F number in hypoxia (2% O₂), suggesting that hypoxic conditions may selectively facilitate the survival of more primitive MSC cells.⁵⁰ It has also been reported that early stage culture in 5% O₂ has a stimulatory effect on rat marrow MSC, as evidenced by significantly increased cell proliferation, decreased apoptosis and necrosis, and decreased expression of hematopoietic markers.⁵¹ Further, it has been shown that hypoxic conditions enhance the osteoblastic^{52,53} and chondrogenic^{54,55} differentiation of bone marrow-derived MSC. The differing effects of hypoxia on MSC phenotype seen in previous studies emphasize the complexity of the progenitor cell microenvironment.

The present study compares the osteogenic and chondrogenic capacity of a mixed cell population (BMMC, which contains MSC, HSC, and EPC) to that of purified, culture-expanded MSC, when encapsulated in a collagen-chitosan hydrogel matrix. It is motivated by the incomplete understanding of how accessory cells and oxygen tension may affect MSC function in the stem cell niche, and how this may translate to therapeutic effect. The BMMC preparation contains cells and biochemical factors that may have paracrine effects on the MSC component of the marrow. In contrast, the MSC preparation is highly purified and therefore has a higher content of mesenchymal progenitor cells, which are known to be responsible for regeneration of orthopedic tissues. Both cell types are embedded in protein-polysaccharide microbeads that enable 3D culture in a controlled and physiologically relevant environment, and the effect of oxygen tension on osteogenic and chondrogenic differentiation is also assessed. This study therefore provides insight into the relative advantages and limitations of fresh marrow suspensions and purified progenitor cell populations for orthopedic repair applications.

Materials and Methods

Rat bone marrow-derived MSC

Four Sprague-Dawley rats (3–6 weeks old) were euthanized using carbon dioxide inhalation prior to harvesting both femur and tibia. The distal and proximal ends of each

femur and tibia were removed and the marrow was flushed out with sterile culture media. A single cell suspension was prepared by mechanical disruption and filtered using a 70- μm cell strainer.⁵⁶ BMMC were plated at 5×10^5 cells/ cm^2 in 75 cm^2 polystyrene cell culture flasks (BD Falcon), and cultured in MSC growth media consisting of α -MEM (Gibco), 10% fetal bovine serum (FBS; HyClone MSC screened), and penicillin (5000 units/100 mL)/streptomycin sulfate (5 mg/100 mL) (P/S; Gibco). Cultures were incubated at 37°C in 20% O₂+5% CO₂ (normoxia). Media were changed every 3–4 days and rat marrow-derived adherent MSC were culture expanded until passage 4, at which point cells were used for hydrogel microbead experiments. Prior to seeding passage 4 MSC into hydrogel microbeads, cell numbers were counted using a Multisizer™ 3 Coulter Counter® (Beckman Coulter).

Freshly isolated uncultured rat BMMC

A single cell suspension was obtained from an additional four Sprague-Dawley rats as outlined above. Red blood cells (RBCs) were lysed using an ammonium chloride-based lysis buffer solution^{57–59} containing 150 mM NH₄Cl (Sigma), 10 mM KHCO₃ (Sigma), and 0.1 mM EDTA (Sigma). A fresh rat bone marrow cell solution in 20 mL of MSC growth media was mixed with 60 mL of RBC lysis buffer (1:3 dilution) for 7 min at room temperature. Cells were centrifuged at 3500 rpm for 2 min, washed with sterile phosphate-buffered saline (PBS), and the collected BMMC were resuspended in 20 mL of MSC growth media. For CFU-F analysis, 150 μL of this BMMC solution was pipetted into a six-well plate and cultured in 20% O₂+5% CO₂ (normoxia) or 5% O₂+10% CO₂ (hypoxia) for 2 weeks with media changes every 3 days, to result in an adherent layer of marrow-derived MSC CFU-F on day 14. These samples were washed with PBS, fixed with 10% buffered formalin (Anatech Ltd.), stained with 1% Toluidine Blue O (Sigma) stain, scanned, and counted for colony number. Prior to directly seeding fresh uncultured BMMC into hydrogel microbeads, BMMC numbers were counted using a Multisizer 3 Coulter Counter, centrifuged at 200g for 5 min, and then resuspended in MSC growth media.

Fabrication of 3D collagen-chitosan hydrogel microbeads containing cells

Collagen-chitosan (mass ratio 65%/35%) hydrogel preparations of 6 mL total initial volume were mixed with each freshly isolated BMMC collection (passage 0, $n=4$) or culture-expanded rat marrow-derived MSC (passage 4, $n=4$). Each collagen-chitosan hydrogel preparation consisted of 3000 μL collagen type 1 (4 mg/mL in 0.02 N acetic acid, from calf skin; MP Biomedicals, cat# 150026, final concentration=2 mg/mL), 330 μL chitosan (2% w/v in 0.1 N acetic acid, Protosan UP B 90/500; FMC BioPolymer/Novamatrix, lot# 1148013, final concentration=0.11% w/v), 730 μL β -glycerophosphate (580 mg/mL in water; Sigma, cat# G9891, final concentration=7.1% w/v=326.7 mM), 70 μL Glyoxal (87.5 mM in water; Sigma, cat# 128465, final concentration=1 mM), and 1870 μL of cell solution in MSC growth media. All components were kept on ice and pipetted together to result in a total volume of 6 mL of collagen-chitosan hydrogel mixture containing cells. Freshly isolated rat marrow-derived BMMC were added into the hydrogel mixture

at an average ($n=4$) concentration of 25.3×10^6 BMMC/mL, whereas culture-expanded marrow-derived MSC (passage 4, $n=4$) were added into the hydrogel mixture at a concentration of 5×10^5 MSC/mL. Microbeads were fabricated by a water-in-oil emulsion method. Briefly, 6 mL of hydrogel-cell mixture was injected at a rate of 6 mL/min into 75 mL of polydimethylsiloxane (PDMS) (PMX-200, 100 cS; Xiameter) under constant stirring using a mixing apparatus (Barnant Co.) with a custom impeller. Emulsification was carried out by mixing at 800 rpm while the PDMS was maintained cold in a crushed ice bath for 5 min. Once the liquid matrix droplets were fully emulsified and homogeneously mixed, the PDMS bath was transferred to a water bath at 37°C for 25 min with constant stirring, to initiate thermal gelation and to achieve co-polymerization of collagen-chitosan microbeads. The resulting cell-encapsulating microbeads were collected from the PDMS phase by centrifugation at 200 g for 5 min and washed thrice with MSC growth media and centrifugation.

Microbead culture in osteogenic or chondrogenic differentiation media in normoxic or hypoxic conditions

Fabricated collagen-chitosan microbeads containing cells were resuspended in 12.0 mL of MSC growth media, and distributed evenly in twelve 15 mL centrifuge tubes by pipetting 1.0 mL of microbead/media solution into each tube and adding an additional 2.0 mL of MSC growth (control) media for culture. Six tubes of cell-microbeads were cultured in 20% O₂+5% CO₂ (normoxia), while the other six tube samples were cultured in 5% O₂+10% CO₂ (hypoxia) for an initial 3 days, with tube caps loosened to allow free gas exchange. Subsequently, culture media were changed for all tube samples by centrifuging at 200 g for 5 min, aspirating media from collected microbeads, and adding 1.5 mL of either MSC growth media, osteogenic differentiation media, or chondrogenic differentiation media to appropriate tube samples. The time point at which these media were added was designated as day 0. Osteogenic differentiation media consisted of control media (α -MEM, 10% FBS, and 1% P/S) supplemented with 0.2 mM L-ascorbic acid 2-phosphate (Sigma), 10 mM β -glycerophosphate (Sigma-Aldrich), and 100 nM dexamethasone (Sigma). Chondrogenic differentiation media consisted of DMEM with high glucose (4.5 mg/mL) and 1 mM sodium pyruvate (Gibco), L-glutamine (4 mM, Gibco), 1% FBS, 1% P/S, 1% ITS+ Universal Culture Supplement Premix (BD Biosciences), 0.2 mM L-ascorbic acid 2-phosphate (Sigma-Aldrich), 0.35 mM L-proline (Sigma), 10 ng/mL rhTGF- β 1 (Peprotech), and 100 nM dexamethasone (Sigma). All culture media were changed every 3 days, by centrifugation of microbeads at 200 g for 5 min, aspiration of used media, and replenishment with 1.5 mL of fresh media. This medium change protocol did not cause any changes in cell viability or morphology.

Imaging and characterization of cell viability and microbeads

At days 1 and 21, cell viability within microbeads was assessed using a commercially available vital staining kit (Live/Dead® Viability/Cytotoxicity Assay Kit; Molecular Probes). A sample of microbeads in 50 μL of culture media (from total of 1.5 mL) was obtained and wash twice in

sterile PBS for 10 min, then incubated at 37°C for 45 min in a solution containing 4.0 μm calcein-AM and 4.0 μm ethidium homodimer-1 in PBS. Briefly, calcein-AM diffuses across the membrane of live cells and reacts with intracellular esterases to emit bright green fluorescence, while ethidium homodimer-1 can enter only dead cells with damaged cell membrane and emit bright red fluorescence upon binding to nucleic acids. After two subsequent PBS washes and resuspension in 100 μL of PBS, microbeads were imaged using laser scanning confocal microscope (Olympus Fluoview™ 500; Olympus America, Inc.). At least three different and random views of dispersed microbeads were imaged at z-resolution of 3 μm , using FITC (ex = 494 nm, em = 517 nm) and PI (528/617 nm) filters. Cell viability in three representative views was quantified using ImageJ Software (National Institutes of Health) to give percentages of live and dead cells from the total number of cells quantified for each sample. Microbead samples at day 21 were imaged with phase contrast using an inverted microscope (Nikon Eclipse Ti-U; Nikon) to show morphology, size, and shade of microbeads.

DNA assay

Microbead samples ($n=4$) were washed with PBS and digested in 275 μL of 1.0 N 50 mM Tris-HCl/4 M Guanidine-HCl buffer (pH=7.5) for 1.5 h at 4°C. A commercially available DNA assay kit (Quanti-iT™ PicoGreen® dsDNA kit; Invitrogen) was used following the manufacturer's protocol to quantify total DNA content from microbead samples. Briefly, duplicate samples of 50 μL of digested sample solution or DNA standards were incubated with 150 μL of 1 \times PicoGreen reagents and then used for fluorescence measurements at 485/518 nm (excitation/emission).

Calcium assay

Microbead samples ($n=4$) were washed with PBS and digested in 275 μL of 1.0 N acetic acid overnight at 4°C. For calcium quantification, an orthocresolphthalein complex one (OCPC) method was used as previously described.^{40,41,60} Briefly, duplicate samples of 50 μL of digested sample solution or calcium standard solution (CaCl_2 ; Sigma) was mixed with 250 μL of working solution consisting of 0.05 mg/mL OCPC solution and ethanolamine/boric acid/8-hydroxyquinoline buffer (Sigma), incubated for 10 min at room temperature, and used for absorbance measurements at 575 nm.

Osteocalcin rat ELISA

Microbeads samples were washed with PBS and digested in 275 μL of 0.2 N HCl overnight, followed by neutralization with 10 N NaOH. A commercially available rat osteocalcin enzyme immunoassay (EIA) kit (Biomedical Technologies, Inc.) was used to quantify total protein content of osteocalcin, a specific protein product of osteoblasts,⁶¹ from microbead samples ($n=4$ for osteogenic, $n=2$ for growth). The sandwich ELISA kit is specific for both carboxylated and decarboxylated rat osteocalcin and was used following the manufacturer's kit protocol. In brief, duplicate samples of 25 μL of digested sample solution or osteocalcin standard were used in the ELISA plate assay, and within 15 min of adding stop solution to all wells, absorbance was measured at 450 nm.

Sulfated glycosaminoglycan/1,9-dimethylmethylene blue assay

Microbeads were washed with PBS and digested overnight at 65°C in 275 μL of papain extraction solution (pH=7.5) consisting of 0.2 M sodium phosphate dibasic (Sigma), 0.1 M sodium acetate (Sigma), 0.01 M disodium EDTA (Sigma), 5 mM L-cysteine HCl monohydrate (Sigma), and 20 $\mu\text{g}/\text{mL}$ of crystallized papain suspension (Sigma). Sulfated glycosaminoglycan (sGAG) from the digested sample solution ($n=4$ for osteogenic and $n=2$ for growth) was measured using a modification of the 1,9-dimethylmethylene blue (DMMB) dye assay developed by Farndale *et al.*⁶² Briefly, duplicate samples of 25 μL of samples and chondroitin sulfate standards (Sigma) were mixed with 200 μL of DMMB (Sigma) dye solution and the absorbance was immediately measured at 525 nm.

Histology

Microbead samples were fixed in Z-Fix (buffered zinc formalin fixative; Anatech Ltd.) for 24 h and stored in 70% ethanol at 4°C. Microbead samples were embedded in collagen-based hydrogel discs using customized Delrin rings of 9.5 mm diameter and 3.2 mm thickness. Briefly, microbeads were mixed with 50 μL of 1 \times DMEM, 50 μL of FBS, 100 μL of 5 \times DMEM, 50 μL of 0.1 NaOH, and 250 μL of collagen type 1 solution (4 mg/mL in 0.02 N acetic acid, from calf skin; MP Biomedicals, cat# 150026, final concentration = 2 mg/mL), while kept on ice. Collagen hydrogel discs were formed by pipetting 200 μL of gel mixture in each ring and incubation at 37°C for 45 min. Gel discs were placed in tissue histology cassettes, fixed for 24 h, and stored in 70% ethanol at 4°C. Microbead-containing gel discs were processed and embedded in paraffin and sectioned at 7 μm . Sections were stained with hematoxylin and eosin (H&E), Alizarin Red S (2%) for calcium deposits, von Kossa (1% silver nitrate, 5% sodium thiosulfate) for phosphate component of mineralization, and safranin-O (0.1%)/fast green (0.05%).

Statistical analyses

Data are reported as mean \pm standard deviation for DNA and calcium assays, to aid in visual appearance of small error bars within these graph figures. Data are reported as mean \pm standard error of the mean for osteocalcin and sGAG assays. Data were analyzed with Student's *t*-test and statistical significance was defined by statistical probability of $p \leq 0.05$.

Results

Characterization of marrow-derived MSC/CFU-F and culture-expanded MSC

Colonies of MSC (MSC/CFU-F) originating from freshly isolated rat BMMC ($n=4$) were plated in wells of a six-well plastic plate, cultured for 14 days in MSC growth media, in either normoxia or hypoxia, and then fixed, stained, and scanned. Numbers of CFU-F from each well image were counted using ImageJ. Compared to the normoxic culture condition (Fig. 1A, average of 39 ± 6 CFU-F), hypoxic culture resulted in a statistically significant ($p=0.04$) increase in CFU-F number (Fig. 1B, average of 66 ± 5 CFU-F).

FIG. 1. Morphology of fresh rat bone marrow-derived mesenchymal stem cells (MSC)/colony-forming unit-fibroblasts (CFU-F) (passage 0) or culture-expanded rat bone marrow-derived culture-expanded MSC (passage 4). CFU-F of MSC originating from freshly isolated rat bone marrow-derived cells cultured for 14 days *in vitro* in (A) 20% oxygen normoxia or (B) 5% oxygen hypoxia. Images were obtained to show morphology of (C) MSC (passage 0) from CFU-F cultured for 14 days in growth media, originating from freshly isolated rat marrow and (D) culture-expanded rat marrow-derived MSC (passage 4) prior to use in hydrogel microbead experiments. Scale bar = 500 μ m. Color images available online at www.liebertpub.com/tea

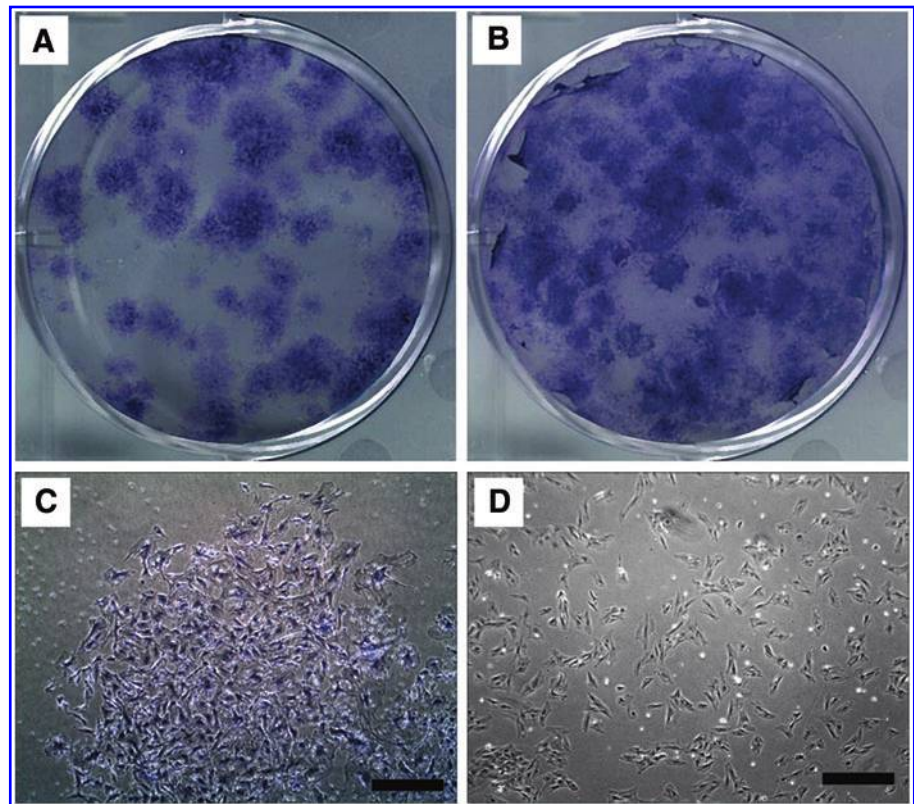
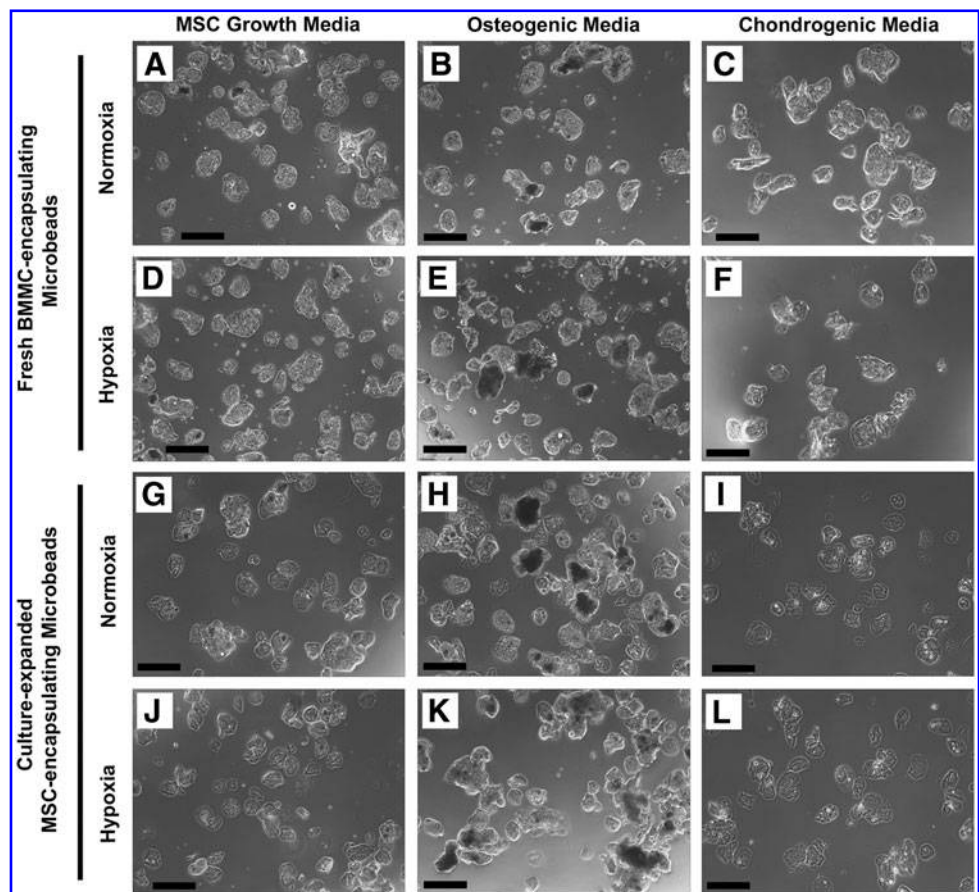


FIG. 2. Phase-contrast images of fresh bone marrow mononuclear cells (BMMC)- or MSC-microbeads at day 21. BMMC-microbeads were cultured in normoxia (A–C) in (A) MSC growth media, (B) osteogenic media, and (C) chondrogenic media, or hypoxia (D–F) in (D) MSC growth media, (E) osteogenic media, and (F) chondrogenic media. MSC-microbeads were cultured in normoxia (G–I) in (G) MSC growth media, (H) osteogenic media, and (I) chondrogenic media, or hypoxia (J–L) in (J) MSC growth media, (K) osteogenic media, and (L) chondrogenic media. Scale bar = 200 μ m.



Cells within a 14-day cultured CFU-F, from the well plate shown in Figure 1A, were imaged with phase-contrast microscopy and showed typical MSC morphology (Fig. 1C). Culture-expanded rat marrow-derived MSC (passage 4) (Fig. 1D) were also imaged with phase-contrast microscopy prior to use in hydrogel microbead experiments. Both fresh marrow-derived MSC and culture-expanded MSC exhibited similar spread, spindle-like or fibroblastic morphologies, on a similar scale.

Morphology of collagen-chitosan microbeads containing cells after 21 days of culture

Collagen-chitosan microbeads encapsulating either fresh BMMC (Fig. 2A–F) or culture-expanded MSC (Fig. 2G–L) and cultured *in vitro* for 21 days were imaged by phase-contrast microscopy. Microbead samples were cultured in normoxic (20% oxygen) or hypoxic (5% oxygen) conditions, in culture media specific for MSC growth, osteogenic differentiation, or chondrogenic differentiation, as indicated in Figure 2. Collagen-chitosan microbeads were generally spheroidal in shape, and microbeads from each sample condition had diameters in the range of ~100–200 μm. No degradation of the microbead matrix was observed and all preparations remained intact over time in culture. Microbeads cultured in osteogenic media were generally more opaque than in other conditions, with a portion appearing notably dark in color, presumably due to mineral deposition.

Cell viability and quantification within microbead samples at day 1 and 21

The proportion of live and dead cells out of the total number of cells quantified in three representative confocal fluorescence image views for each sample condition on day 1 and 21 are summarized in Table 1. Representative confocal fluorescence images of cell viability for BMMC-microbeads at day 1 (Fig. 3A–F) and day 21 (Fig. 4A–F), and for MSC-microbeads at day 1 (Fig. 3G–L) and day 21 (Fig. 4G–L) were obtained.

BMMC-microbeads cultured in normoxia (Fig. 3A–C) at day 1 in growth, osteogenic, and chondrogenic media contained a mixture of live (green) and dead (red) cells (32%–42% viable), whereas BMMC-microbeads cultured in hypoxia (Fig. 3D–F) contained notably more live cells than dead cells (51%–57% viable). Cell viability in MSC-microbeads cultured in normoxia and hypoxia at day 1 in growth, osteogenic, and chondrogenic media was uniformly high (83%–94% viable) (Fig. 3G–L). The majority of all cells encapsulated in collagen-chitosan microbeads at day 1 (Fig. 3) have a rounded morphology, although some cells can be observed as slightly spread, particularly in the samples with culture-expanded MSC.

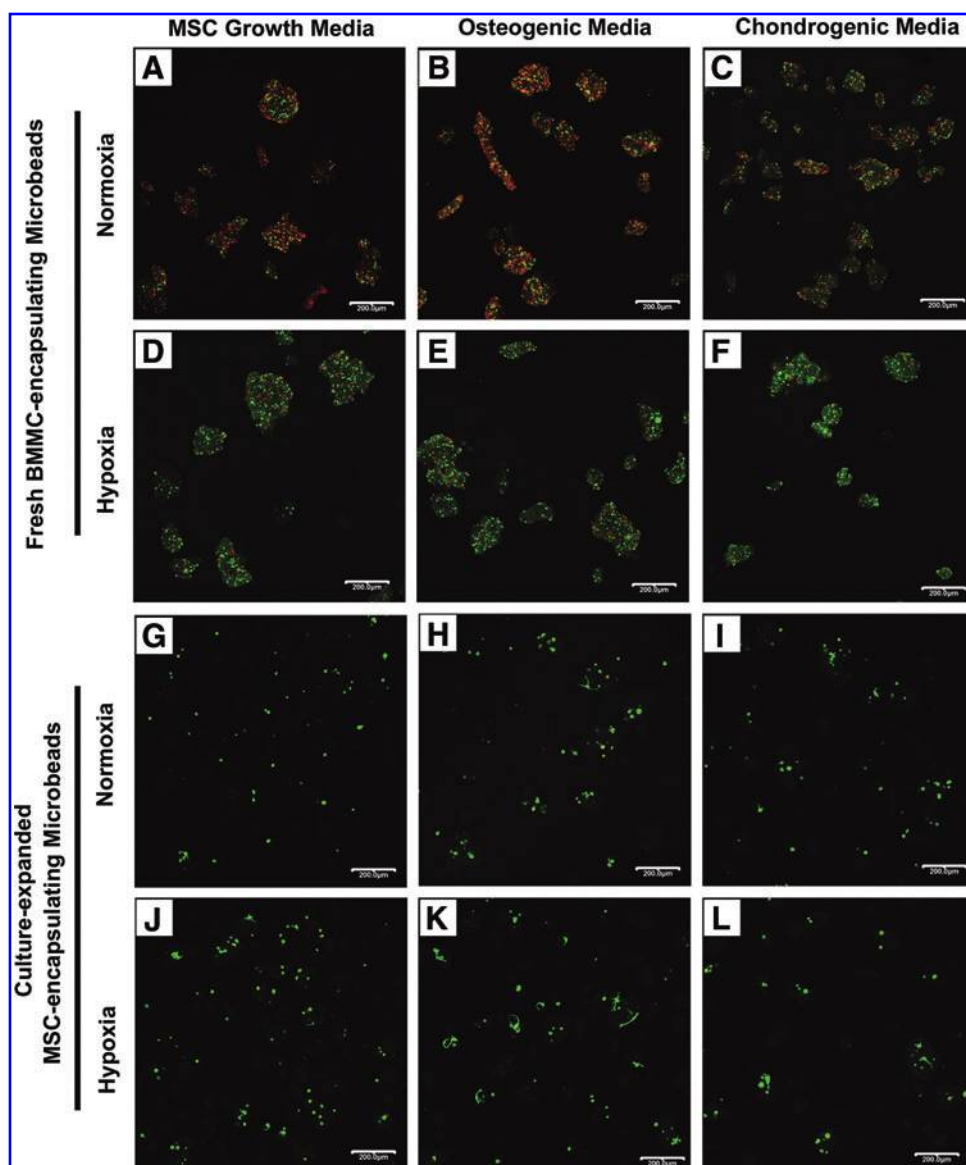
At day 21, the proportion of living cells in BMMC-microbeads cultured in growth or osteogenic media, either in normoxia or hypoxia, markedly increased to 61%–85% (Fig. 4A–E), depending on condition. Spreading of live cells within the collagen-chitosan microbeads was evident in the growth media/hypoxia (Fig. 4D), osteogenic/normoxia (Fig. 4B), and osteogenic/hypoxia (Fig. 4E) conditions. Cells in the growth media/normoxic (Fig. 4A) condition remained rounded. Interestingly, BMMC-microbeads cultured for 21 days in chondrogenic media exhibited very marked cell death, with only 3% viable cells in normoxia (Fig. 4C), and a slightly higher number of rounded viable

TABLE 1. QUANTIFICATION OF CELL VIABILITY IN MICROBEAD SAMPLES

	MSC growth media	% Live cells	% Dead cells	Total no. of cells	Osteogenic media	% Live cells	% Dead cells	Total no. of cells	Chondrogenic media	% Live cells	% Dead cells	Total no. of cells
Day 1	BMMCs normoxia	35	65	871	BMMCs normoxia	32	68	1071	BMMCs normoxia	42	58	1078
	BMMCs hypoxia	57	43	1062	BMMCs hypoxia	51	49	1108	BMMCs hypoxia	57	43	594
	MSCs normoxia	94	6	212	MSCs normoxia	84	16	178	MSCs normoxia	88	12	147
Day 21	MSCs hypoxia	83	17	265	MSCs hypoxia	90	10	240	MSCs hypoxia	80	20	113
	BMMCs normoxia	61	39	774	BMMCs normoxia	79	21	1020	BMMCs normoxia	3	98	890
	BMMCs hypoxia	64	36	756	BMMCs hypoxia	85	15	462	BMMCs hypoxia	13	87	897
	MSCs normoxia	72	28	267	MSCs normoxia	94	6	381	MSCs normoxia	87	13	220
	MSCs hypoxia	83	17	485	MSCs hypoxia	91	9	774	MSCs hypoxia	92	8	206

Percentages of live and dead cells out of the total number of cells were quantified from three representative fluorescence confocal images. Microbead samples were cultured for 1 or 21 days in growth, osteogenic, or chondrogenic media, and either in normoxia or hypoxia. MSC, mesenchymal stem cells; BMMC, bone marrow mononuclear cells.

FIG. 3. Cell viability of fresh BMMC- and MSC-microbeads at day 1. BMMC-microbeads were cultured in normoxia (A–C) in (A) MSC growth media, (B) osteogenic media, and (C) chondrogenic media, or hypoxia (D–F) in (D) MSC growth media, (E) osteogenic media, and (F) chondrogenic media. MSC-microbeads were cultured in normoxia (G–I) in (G) MSC growth media, (H) osteogenic media, and (I) chondrogenic media, or hypoxia (J–L) in (J) MSC growth media, (K) osteogenic media, and (L) chondrogenic media. Scale bar = 200 μ m. Images best viewed in color. Color images available online at www.liebertpub.com/tea



cells (13%) in hypoxia (Fig. 4F). In contrast, cell viability in MSC-microbeads at day 21 (Fig. 4G–L) remained high (72%–94% viable) under all culture conditions. Cell spreading within the collagen-chitosan microbead matrix was more evident in growth (Fig. 4G, J) and osteogenic media cultures (Fig. 4H, K).

Quantification of total DNA content in microbeads

Figure 5 shows the total DNA content measured in BMMC- or MSC-microbeads cultured in control MSC growth media (Fig. 5A or D), osteogenic media (Fig. 5B or E), or chondrogenic media (Fig. 5C or F), either in normoxia or hypoxia. At day 1, BMMC-microbeads cultured in normoxia contained the highest DNA content, whereas BMMC-microbeads cultured in hypoxia showed significantly reduced DNA content, compared to normoxia (Fig. 5A–C). All MSC-microbeads (Fig. 5D–F) contained a much lower DNA content (<10 μ g) than BMMC-microbeads because the purified cells were seeded at a much lower total

cell concentration (5.0×10^5 cells/mL) than the fresh marrow preparation (25.3×10^6 cells/mL). By day 21, BMMC-microbeads cultured in all media and oxygen conditions exhibited a marked reduction in DNA, relative to day 1 (Fig. 5A–C). There was no significant change in average DNA content in MSC-microbeads, compared to day 1 samples (Fig. 5D–F).

Quantification of total calcium content from microbead samples

Figure 6 shows the total calcium content measured in BMMC- or MSC-microbeads, cultured in normoxia or hypoxia, in control MSC growth media (Fig. 6A), osteogenic media (Fig. 6B), or chondrogenic media (Fig. 6C). At day 1, all samples exhibited calcium levels less than 200 μ g. There was a time-dependent increase in calcium, regardless of oxygen status, for microbeads cultured for 21 days under control or osteogenic conditions, which displayed marked increases in calcium content (into the range of 400–500 μ g), compared with day 1. In contrast, microbead samples

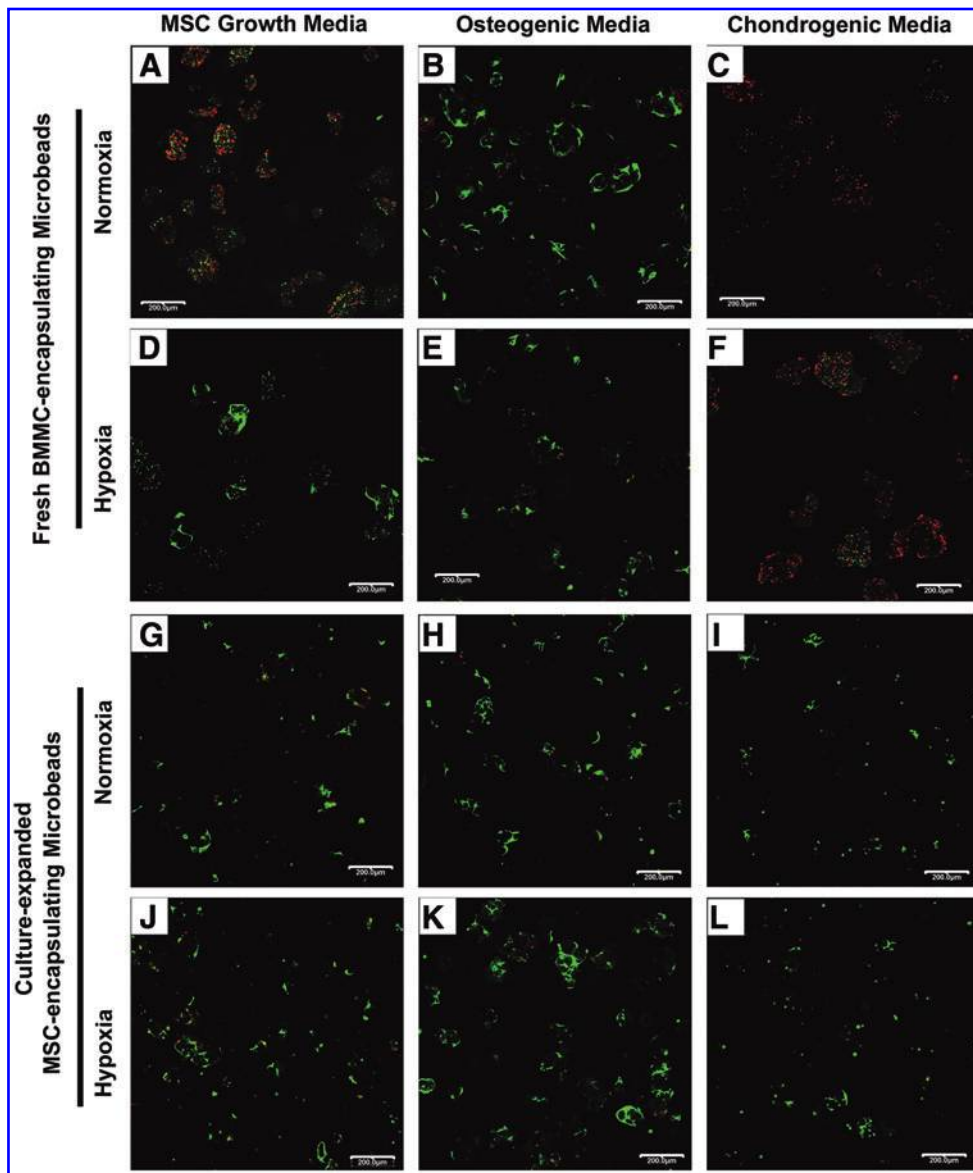


FIG. 4. Cell viability of BMMC-microbeads and MSC-microbeads at day 21. BMMC-microbeads were cultured in normoxia (A–C) in (A) MSC growth media, (B) osteogenic media, and (C) chondrogenic media, or hypoxia (D–F) in (D) MSC growth media, (E) osteogenic media, and (F) chondrogenic media. MSC-microbeads were cultured in normoxia (G–I) in (G) MSC growth media, (H) osteogenic media, and (I) chondrogenic media, or hypoxia (J–L) in (J) MSC growth media, (K) osteogenic media, and (L) chondrogenic media. Scale bar = 200 μm . Images best viewed in color. Color images available online at www.liebertpub.com/tea

cultured in chondrogenic media did result in statistically significant change in calcium levels, compared with day 1. Calcium levels in osteogenic media were not different from those in control media at day 21.

Quantification of total osteocalcin protein from microbead samples

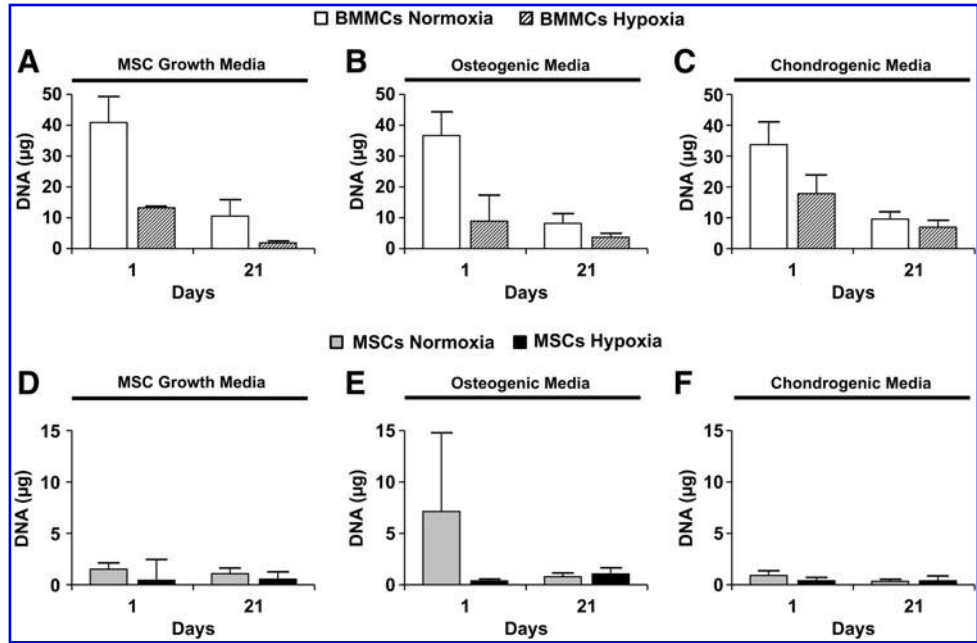
Figure 7 shows the total osteocalcin protein content (in ng) measured in BMMC- and MSC-microbeads cultured in either control MSC growth media (Fig. 7A) or osteogenic media (Fig. 7B), in either normoxia or hypoxia. In BMMC-microbeads, initial osteocalcin levels at day 1 were maintained until day 21, regardless of oxygen status. (Fig. 7A, B). MSC-microbeads cultured in control media (Fig. 7A) in either normoxic or hypoxic conditions exhibited a significant increase in osteocalcin from day 1 to 21, while those microbeads cultured in osteogenic media (Fig. 7B) did not show a statistically significant osteocalcin level increase. Osteocalcin levels in BMMC-microbeads and MSC-microbeads

cultured in control media were not statistically different from each other (in the range of 300–400 ng) at day 21.

Quantification of total sGAG from microbead samples

Figure 8 shows the total sGAG content measured in BMMC- and MSC-microbeads cultured in normoxia or hypoxia, in either control MSC growth media (Fig. 8A) or chondrogenic media (Fig. 8B). There were no significant increases in sGAG levels by day 21, relative to day 1, for any microbead culture condition. BMMC-microbeads cultured for 21 days in control media (Fig. 8A) or chondrogenic media (Fig. 8B), regardless of oxygen status, resulted in significantly higher amounts of total sGAG content, compared with MSC-microbeads. However, it should be noted that cell viability in day 21 samples varied greatly, as shown in Table 1. In particular, the cells within BMMC-microbeads cultured in control media were at least 61% alive at day 21, whereas the majority of cells cultured in chondrogenic media were not viable. The cells in

FIG. 5. Total DNA content from microbead samples. BMMC-microbead samples were cultured in (A) MSC growth media ($n=4$), (B) osteogenic media ($n=4$), or (C) chondrogenic media ($n=4$). MSC-microbead samples were cultured in (D) MSC growth media ($n=4$), (E) osteogenic media ($n=4$), or (F) chondrogenic media ($n=4$). Bars represent mean \pm standard deviation (SD).



MSC-microbeads maintained their viability at about 70% in all conditions at day 21.

Histology

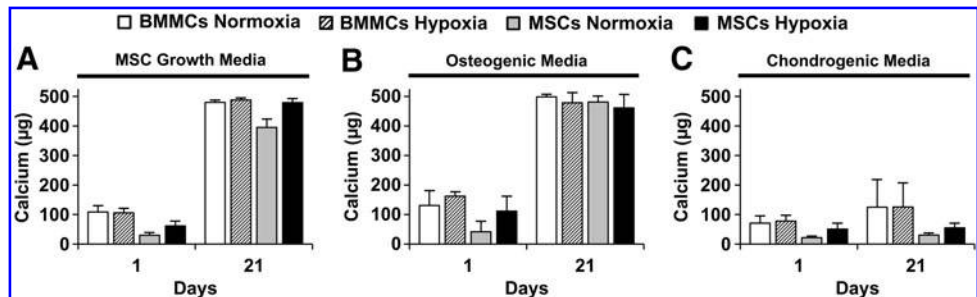
BMMC- and MSC-microbeads cultured in normoxia or hypoxia, and cultured in control MSC growth media, osteogenic media, or chondrogenic media, were sectioned and stained with H&E, Alizarin Red, von Kossa stain, and safranin-O/fast green. Eosin stained the microbead matrix pink, and hematoxylin stained cell nuclei blue. Little to no staining with Alizarin Red or von Kossa, indicative of calcium deposits and phosphate mineralization, was observed in BMMC-microbeads or MSC-microbeads cultured in control MSC growth media for 21 days (Fig. 9A, C), either in normoxic or hypoxic conditions. In contrast, strong positive staining for Alizarin Red and von Kossa was displayed by both BMMC-microbeads and MSC-microbeads cultured in osteogenic media for 21 days (Fig. 9B, D), either in normoxia or hypoxia. The calcium assay using OCPC method (Fig. 6) reacts with calcium ions, whereas the Alizarin Red S staining reacts with calcium salts (calcium phosphate and calcium carbonate) in histological tissue sections. Although the results of the OCPC calcium assay display similar high levels of calcium for samples cultured in either growth media or osteogenic media for 21 days, strong staining by

Alizarin Red S was evident in samples cultured in osteogenic media, but not samples cultured in MSC growth media. This result suggests that osteogenic supplements in media are necessary for the formation of true mineral deposits containing both calcium and phosphate. Microbeads cultured in any condition did not stain positive for safranin-O (not shown), and microbeads cultured in chondrogenic media showed no presence of Alizarin Red or von Kossa staining (not shown).

Discussion

The major objective of this work was to compare the osteogenic and chondrogenic potential of fresh uncultured BMMC to that of purified, culture-expanded MSC when encapsulated in 3D collagen-chitosan microbeads. Our overall hypothesis was that the varied and potent mixture of cells that make up marrow would have positive effects on the relatively small MSC fraction, and in particular would potentiate their ability to undergo osteogenesis when embedded in 3D collagen-chitosan matrices. Interestingly, our study showed that fresh uncultured BMMC exhibited a similar degree of osteogenesis as culture-expanded MSC when cultured in collagen-chitosan microbeads for 21 days, as assessed by calcium deposition, osteocalcin expression, and histological analysis. However, chondrogenic potential

FIG. 6. Total calcium content from microbead samples. Microbead samples were cultured in (A) MSC growth media ($n=4$), (B) osteogenic media ($n=4$), or (C) chondrogenic media ($n=4$). Bars represent mean \pm SD.



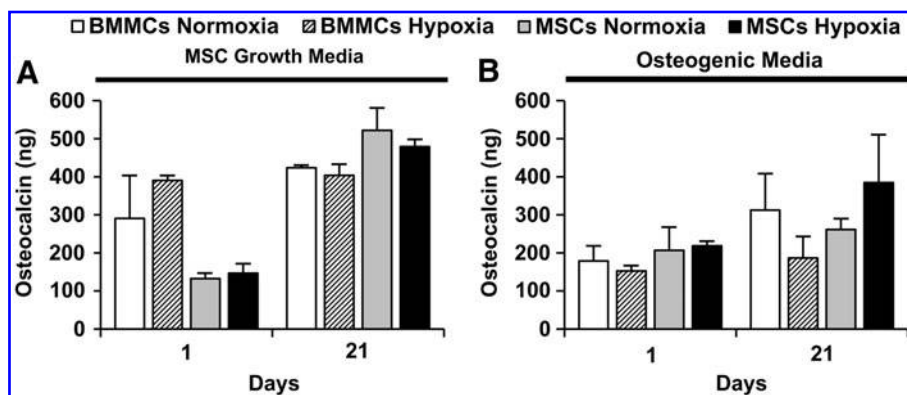


FIG. 7. Total osteocalcin protein from microbead samples. Microbead samples were cultured in either (A) MSC growth media ($n=2$) or (B) osteogenic media ($n=4$). Bars represent mean \pm standard error of the mean (SEM).

was not supported for either cell preparation type in collagen-chitosan microbeads over 21 days.

Differential counts reveal that the cells in normal rat bone marrow include myeloid cells ($\approx 44\%$), erythroid cells ($\approx 36\%$), lymphocytes ($\approx 19\%$), and plasma cells ($\approx 0.4\%$).⁶³ The abundant RBC fraction may inhibit nutrition and initial proliferation of MSC, and therefore we used an ammonium chloride buffer solution to lyse and remove the majority of erythrocytes from the fresh marrow isolate, which may also result in more remaining platelets and platelet-derived growth factor.⁵⁵⁻⁵⁷ The remaining BMMC preparation therefore consisted of a heterogeneous population of cells, including MSC, HSC/HPC, EPC, adipocytes, macrophages, monocytes, neutrophils, and platelets. These components can secrete a variety of cytokines and growth factors, and may work in concert through paracrine signaling to enhance bone formation.⁶⁴ In particular, it has been reported that HSC and other hematopoietic-lineage cells can enhance survival and proliferation of bone marrow-derived CFU-F and CFU-O *in vitro*,^{24,65} and significantly stimulate osteogenesis.²⁴⁻²⁵

MSC are a rare population of cells within human bone marrow. Their frequency is reported to be in the range of 0.01%–0.001% of BMMC,^{1,5,30} although the clonogenicity of human marrow aspirates can be variable and significantly correlated to the age of the donor.^{30,66} In the present work, the prevalence of MSC in rat marrow was found to be about 0.002%. Therefore, the overall conclusion from this study that fresh BMMC-microbeads and culture-expanded MSC-microbeads exhibit a similar extent of osteogenic potential is remarkable, since the heterogeneous BMMC group contained only about 1/10th the number of MSC as the purified MSC

group. These results suggest that there is a synergistic effect between the non-MSC component of the BMMC preparation and the small MSC fraction. Our data suggest that the number of MSC in both microbead types increased over time in culture, while the non-MSC fraction decreased. The relative influence of proliferation and potentiation of differentiation on osteogenesis was not independently examined, however it was clear that the presence of the supporting cells of BMMC played a role in improving osteogenic function.

This study also examined the effect of low oxygen tension (5%), relative to the standard level of oxygen *in vitro* (20%) on cell encapsulation and function. Hypoxia significantly increased initial colony number derived from freshly isolated rat BMMC. In microbeads, it was observed that hypoxia enhanced initial survival and number of bone marrow progenitor cells, but did not enhance osteogenic or chondrogenic potential in either BMMC- or MSC-microbeads. Hypoxic culture has been shown to enhance chondrogenic differentiation of MSC,⁵⁴⁻⁵⁵ but the effects of hypoxic culture on osteogenic differentiation are still not fully understood, and are highly dependent on the concentration of oxygen, duration of hypoxia, and source and cell seeding densities of MSC, and other factors. Several studies have suggested that hypoxic culture inhibits osteogenic differentiation of MSC,⁶⁷⁻⁷¹ while others have determined that hypoxia can enhance osteogenic differentiation of MSC.^{47,52,53} Our results indicate that initial hypoxic culture (first 4 days) of freshly isolated BMMC can enhance the survival and proliferation of fresh MSC, but that longer term (21 days) constant hypoxia may not be beneficial to osteogenic differentiation. The timing and duration of hypoxic culture of freshly isolated BMMC must be

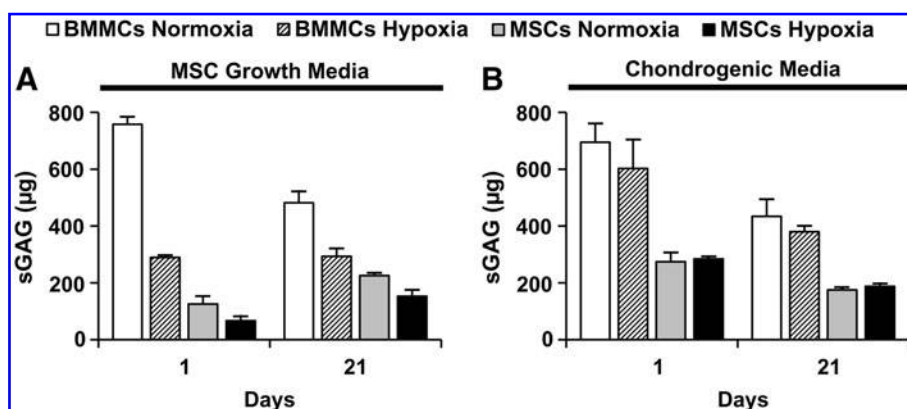


FIG. 8. Total Sulfated glycosaminoglycan (sGAG) from microbead samples. Microbead samples were cultured in either (A) MSC growth media ($n=2$) or (B) chondrogenic media ($n=4$). Bars represent mean \pm SEM.

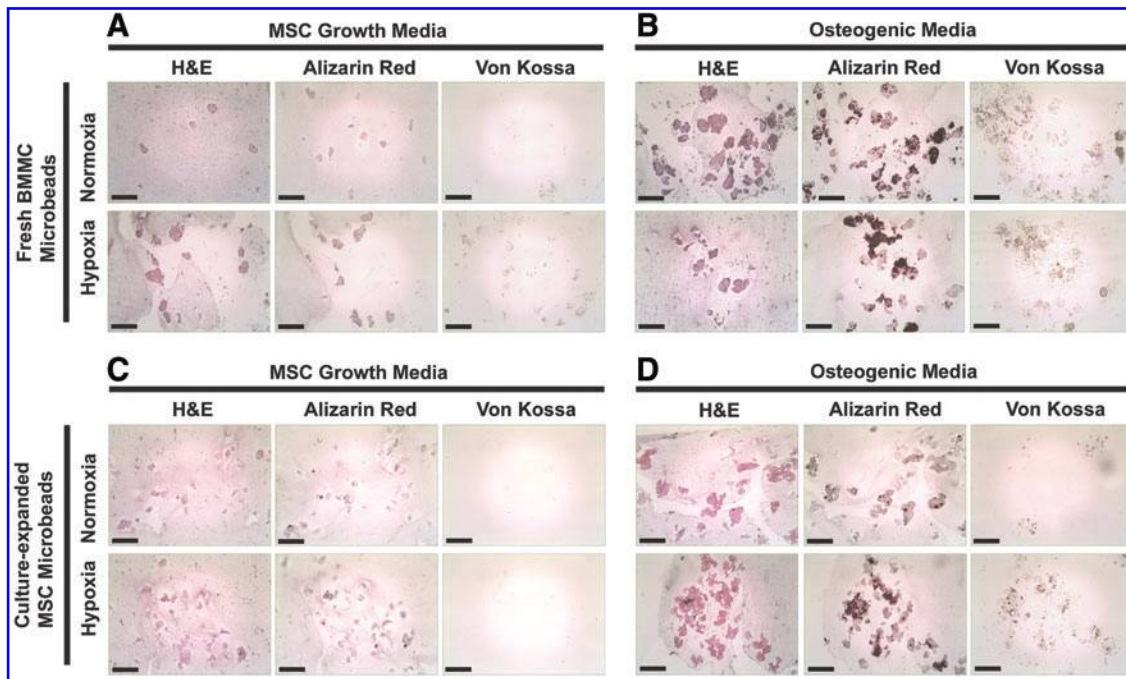


FIG. 9. Histology. Sections (7 μm) of BMMC-microbeads cultured in (A) MSC growth media or (B) osteogenic media, or MSC-microbeads cultured in (C) MSC growth media or (D) osteogenic media, for 21 days either in normoxia or hypoxia. Sections were stained with hematoxylin and eosin (H&E), Alizarin Red S, or von Kossa. Scale bar = 200 μm . Images best viewed in color. Color images available online at www.liebertpub.com/tea

considered in future studies for optimal osteogenic and chondrogenic differentiation.

Under the conditions tested in this study, neither BMMC- nor MSC-microbeads supported chondrogenesis. One reason for this finding may have been the low MSC seeding density that was used, relative to most studies investigating 3D chondrogenesis using progenitor cells. It has been reported that chondrogenic differentiation, specifically within collagen-based microspheres, requires a high cell seeding density to promote required cell-cell interactions and significant sGAG deposition.^{44,72} We seeded culture-expanded MSC at a concentration of 5×10^5 cells/mL, and the estimated initial concentration of MSC in the fresh BMMC preparation was about 5×10^4 cells/mL. These cell concentrations are at least an order of magnitude lower than the values typically used in pellet culture and other forms of high density cartilage tissue engineering. This issue complicates the use of fresh BMMC preparations for cartilage applications, though it should be noted that whole or concentrated uncultured bone marrow has been used to successfully repair osteochondral defects.⁷³ Another reason for the lack of chondrogenesis in our study may have been the matrix formulation, which consisted of 35% chitosan and 65% collagen Type I. Chitosan has structural properties similar to cartilage-specific GAG, and chitosan-based scaffolds have been shown to be supportive of chondrogenic differentiation of MSC.⁷⁴⁻⁷⁵ However, the molecular weight, degree of deacetylation, viscosity, and concentration of chitosan are likely to be important factors in determining the survival, proliferation, and chondrogenic differentiation of MSC in such hydrogels. Alginate, another polysaccharide material used for tissue engineering, has been shown to support chondrogenesis of MSC both *in vitro*⁷⁶⁻⁷⁸ and *in vivo*.⁷⁹ Collagen Type I is not a

main component of normal hyaline cartilage, and collagen Type II is more typically associated with this tissue. It has been reported that collagen Type II hydrogels resulted in the more prominent chondrogenic differentiation of MSC,⁸⁰ compared to alginate or collagen Type I. Further, collagen Type II coatings on alginate microbeads⁸¹ or chitosan fibrous scaffolds⁸² can enhance MSC proliferation and chondrogenesis. It is likely that a higher MSC concentration and a matrix formulation more conducive to chondrogenesis would be required to create microbeads for cartilage tissue engineering.

The hydrogel microbead format offers several advantages for encapsulation, culture, and delivery of progenitor cells for orthopedic tissue engineering. In the case of freshly isolated BMMC, the freshly harvested marrow cells can be directly embedded within 3D protein microbeads without being exposed to 2D adherent culture, which can negatively affect progenitor cell properties. Purified MSC can be expanded in 2D culture, but can then also be embedded in microbeads for further culture in a more physiological environment. The microbeads used in this study were fabricated to have diameters in the range 100–200 μm , which ensures that the maximum diffusion length for nutrients and oxygen to the cells is at most 100 μm , well within the range found in metabolically active tissues.⁸³ Batches of cell-encapsulating collagen-chitosan microbeads can be easily fabricated by emulsification, cultured in suspension, and then collected for cell delivery. Concentration of microbead preparations produces cohesive pastes or constructs that can be formed into a variety of shapes and sizes, and can be tailored to fit a specific defect.³⁸ Our choice of a 35% chitosan/65% collagen matrix in this study reflects the established value of these materials in orthopedic tissue engineering, and resulted in robust and stable microbeads

that retained their morphology over time in culture. In particular, the collagen component provides contact with a native ECM protein that regulates the adhesion, proliferation, and differentiation of MSC.^{35,36,42–44,46,84,85} Chitosan is a naturally derived polysaccharide that provides mechanical stability to the microbeads, and it also has been widely used in orthopedic applications.^{40,41,86,87}

In conclusion, this study has demonstrated that both unpurified fresh bone marrow preparations, and purified and culture-expanded MSC can be encapsulated in protein-polysaccharide microbeads. Further, the data show that unpurified BMMC have osteogenic potential similar to that of purified MSC, even though the unpurified preparations initially contain far fewer mesenchymal progenitor cells. These results suggest new approaches to treating bone defects, and in particular those that may benefit from the paracrine contribution of the totality of the cells in marrow, for example, in cases where robust vascularization is required to promote healing. Future studies will include evaluation of the bone regeneration capability of such microbeads in relevant bone defect models *in vivo*.

Acknowledgments

These studies were funded in part by the “Large Bone Defect Healing (LBDH)” Collaborative Research Center of the AO Foundation. The Microscope and Image Analysis Laboratories (MIL) facility at the University of Michigan provided assistance with laser scanning confocal microscopy. John Baker at the Histology Unit of the Orthopedic Research Laboratories at the University Michigan provided assistance with histology.

Disclosure Statement

No competing financial interests exist.

References

- Friedenstein, A.J., Chailakhyan, R.K., and Gerasimov, U.V. Bone marrow osteogenic stem cells: *in vitro* cultivation and transplantation in diffusion chambers. *Cell Tissue Kinet* **20**, 263, 1987.
- Haynesworth, S.E., Goshima, J., Goldberg, V.M., and Caplan, A.I. Characterization of cells with osteogenic potential from human marrow. *Bone* **13**, 81, 1992.
- Bruder, S.P., Jaiswal, N., and Haynesworth, S.E. Growth kinetics, self-renewal, and the osteogenic potential of purified human mesenchymal stem cells during extensive subcultivation and following cryopreservation. *J Cell Biochem* **64**, 278, 1997.
- Prockop, D.J. Marrow stromal cells as stem cells for non-hematopoietic tissues. *Science* **276**, 71, 1997.
- Pittenger, M.F., Mackay, A.M., Beck, S.C., Jaiswal, R.K., Douglas, R., Mosca, J.D., Moorman, M.A., Simonetti, D.W., Craig, S., and Marshak, D.R. Multilineage potential of adult human mesenchymal stem cells. *Science* **284**, 143, 1999.
- Bianco, P., Riminucci, M., Gronthos, S., and Robey, P.G. Bone marrow stromal stem cells: nature, biology, and potential applications. *Stem Cells* **3**, 180, 2001.
- Caplan, A.I., and Dennis, J.E. Mesenchymal stem cells as trophic mediators. *J Cell Biochem* **98**, 1076, 2006.
- Nauta, A.J., and Fibbe, W.E. Immunomodulatory properties of mesenchymal stromal cells. *Blood* **110**, 3499, 2007.
- Salem, H.K., and Thiernemann, C. Mesenchymal stromal cells: current understanding and clinical status. *Stem Cells* **28**, 585, 2010.
- Boquest, A.C., Shahdadfar, A., Frønsdal, K., Sigurjonsson, O., Tunheim, S.H., Collas, P., and Brinckmann, J.E. Isolation and transcription profiling of purified uncultured human stromal stem cells: alteration of gene expression after *in vitro* cell culture. *Mol Biol Cell* **16**, 1131, 2005.
- Boiret, N., Rapatel, C., Veyrat-Masson, R., Guillouard, L., Guérin, J.J., Pigeon, P., Descamps, S., Boisgard, S., and Berger, M.G. Characterization of nonexpanded mesenchymal progenitor cells from normal adult human bone marrow. *Exp Hematol* **33**, 219, 2005.
- Boos, A.M., Loew, J.S., Deschler, G., Arkudas, A., Bleiziffer, O., Gulle, H., Dragu, A., Kneser, U., Horch, R.E., and Beier, J.P. Directly auto-transplanted mesenchymal stem cells induce bone formation in a ceramic bone substitute in an ectopic sheep model. *J Cell Mol Med* **15**, 1364, 2011.
- Mödder, U.I., Roforth, M.M., Nicks, K.M., Peterson, J.M., McCready, L.K., Monroe, D.G., and Khosla, S. Characterization of mesenchymal progenitor cells isolated from human bone marrow by negative selection. *Bone* **50**, 804, 2012.
- Qian, H., Le Blanc, K., and Sigvardsson, M. Primary mesenchymal stem and progenitor cells from bone marrow lack expression of CD44 protein. *J Biol Chem* **287**, 25795, 2012.
- Rombouts, W.J., and Ploemacher, R.E. Primary murine MSC show highly efficient homing to the bone marrow but lose homing ability following culture. *Leukemia* **17**, 160, 2003.
- Wynn, R.F., Hart, C.A., Corradi-Perini, C., O'Neill, L., Evans, C.A., Wraith, J.E., Fairbairn, L.J., and Bellantuono, I. A small proportion of mesenchymal stem cells strongly expresses functionally active CXCR4 receptor capable of promoting migration to bone marrow. *Blood* **104**, 2643, 2004.
- Honczarenko, M., Le, Y., Swierkowski, M., Ghiran, I., Glodek, A.M., and Silberstein, L.E. Human bone marrow stromal cells express a distinct set of biologically functional chemokine receptors. *Stem Cells* **24**, 1030, 2006.
- Son, B.R., Marquez-Curtis, L.A., Kucia, M., Wysoczynski, M., Turner, A.R., Ratajczak, J., Ratajczak, M.Z., and Janowska-Wieczorek, A. Migration of bone marrow and cord blood mesenchymal stem cells *in vitro* is regulated by stromal-derived factor-1-CXCR4 and hepatocyte growth factor-c-met axes and involves matrix metalloproteinases. *Stem Cells* **24**, 1254, 2006.
- Potapova, I.A., Brink, P.R., Cohen, I.S., and Doronin, S.V. Culturing of human mesenchymal stem cells as three-dimensional aggregates induces functional expression of CXCR4 that regulates adhesion to endothelial cells. *J Biol Chem* **283**, 13100, 2008.
- Banfi, A., Muraglia, A., Dozin, B., Mastrogiacomo, M., Cancedda, R., and Quarto, R. Proliferation kinetics and differentiation potential of *ex vivo* expanded human bone marrow stromal cells: implications for their use in cell therapy. *Exp Hematol* **28**, 707, 2000.
- Mendes, S.C., Tibbe, J.M., Veenhof, M., Bakker, K., Both, S., Platenburg, P.P., Oner, F.C., de Bruijn, J.D., and van Blitterswijk, C.A. Bone tissue-engineered implants using human bone marrow stromal cells: effect of culture conditions and donor age. *Tissue Eng* **8**, 911, 2002.
- Alves, H., Munoz-Najar, U., De Wit, J., Renard, A.J., Hoeijmakers, J.H., Sedivy, J.M., Van Blitterswijk, C., and De Boer, J. A link between the accumulation of DNA damage and loss of multi-potency of human mesenchymal stromal cells. *J Cell Mol Med* **14**, 2729, 2010.

23. Aubin, J.E. Osteoprogenitor cell frequency in rat bone marrow stromal populations: role for heterotypic cell-cell interactions in osteoblast differentiation. *J Cell Biochem* **72**, 396, 1999.
24. Baksh, D., Davies, J.E., and Zandstra, P.W. Soluble factor cross-talk between human bone marrow-derived hematopoietic and mesenchymal cells enhances *in vitro* CFU-F and CFU-O growth and reveals heterogeneity in the mesenchymal progenitor cell compartment. *Blood* **106**, 3012, 2005.
25. Jung, Y., Song, J., Shiozawa, Y., Wang, J., Wang, Z., Williams, B., Havens, A., Schneider, A., Ge, C., Franceschi, R.T., McCauley, L.K., Krebsbach, P.H., and Taichman, R.S. Hematopoietic stem cells regulate mesenchymal stromal cell induction into osteoblasts thereby participating in the formation of the stem cell niche. *Stem Cells* **26**, 2042, 2008.
26. Khosla, S., Westendorf, J.J., and Mödder, U.I. Concise review: insights from normal bone remodeling and stem cell-based therapies for bone repair. *Stem Cells* **28**, 2124, 2010.
27. Kretlow, J.D., Spicer, P.P., Jansen, J.A., Vacanti, C.A., Kasper, F.K., and Mikos, A.G. Uncultured marrow mononuclear cells delivered within fibrin glue hydrogels to porous scaffolds enhance bone regeneration within critical-sized rat cranial defects. *Tissue Eng Part A* **16**, 3555, 2010.
28. Braccini, A., Wendt, D., Jaquiere, C., Jakob, M., Heberer, M., Kenins, L., Wodnar-Filipowicz, A., Quarto, R., and Martin, I. Three-dimensional perfusion culture of human bone marrow cells and generation of osteoinductive grafts. *Stem Cells* **23**, 1066, 2005.
29. Scaglione, S., Braccini, A., Wendt, D., Jaquiere, C., Beltrame, F., Quarto, R., and Martin, I. Engineering of osteoinductive grafts by isolation and expansion of ovine bone marrow stromal cells directly on 3D ceramic scaffolds. *Biotechnol Bioeng* **83**, 181, 2006.
30. Braccini, A., Wendt, D., Farhadi, J., Schaeren, S., Heberer, M., and Martin, I. The osteogenicity of implanted engineered bone constructs is related to the density of clonogenic bone marrow stromal cells. *J Tissue Eng Regen Med* **1**, 60, 2007.
31. Chatterjea, A., Renard, A.J., Jolink, C., van Blitterswijk, C.A., and de Boer, J. Streamlining the generation of an osteogenic graft by 3D culture of unprocessed bone marrow on ceramic scaffolds. *J Tissue Eng Regen Med* **6**, 103, 2012.
32. Ye, X., Yin, X., Yang, D., Tan, J., and Liu, G. Ectopic bone regeneration by human bone marrow mononucleated cells, undifferentiated and osteogenically differentiated bone marrow mesenchymal stem cells in beta-tricalcium phosphate scaffolds. *Tissue Eng Part C Methods* **18**, 545, 2012.
33. Chang, F., Ishii, T., Yanai, T., Mishima, H., Akaogi, H., Ogawa, T., and Ochiai, N. Repair of large full-thickness articular cartilage defects by transplantation of autologous uncultured bone-marrow-derived mononuclear cells. *J Orthop Res* **26**, 18, 2008.
34. Zhang, Y., Wang, F., Chen, J., Ning, Z., and Yang, L. Bone marrow-derived mesenchymal stem cells versus bone marrow nucleated cells in the treatment of chondral defects. *Int Orthop* **36**, 1079, 2012.
35. Lund, A.W., Bush, J.A., Plopper, G.E., and Stegemann, J.P. Osteogenic differentiation of mesenchymal stem cells in defined protein beads. *J Biomed Mater Res B Appl Biomater* **87**, 213, 2008.
36. Lund, A.W., Yener, B., Stegemann, J.P., and Plopper, G.E. The natural and engineered 3D microenvironment as a regulatory cue during stem cell fate determination. *Tissue Eng Part B Rev* **15**, 371, 2009.
37. Chen, Z., Wang, L., and Stegemann, J.P. Phase-separated chitosan-fibrin microbeads for cell delivery. *J Microencapsul* **28**, 344, 2011.
38. Caldwell, D.J., Rao, R.R., and Stegemann, J.P. Assembly of discrete collagen-chitosan microenvironments into multiphase tissue constructs. *Adv Healthc Mater* **2**, 673, 2013.
39. Wang, L., Rao, R.R., and Stegemann, J.P. Delivery of mesenchymal stem cells in chitosan/collagen microbeads for orthopedic tissue repair. *Cells Tissues Organs* **197**, 333, 2013.
40. Wang, L., and Stegemann, J.P. Thermogelling chitosan and collagen composite hydrogels initiated with beta-glycerophosphate for bone tissue engineering. *Biomaterials* **31**, 3976, 2010.
41. Wang, L., and Stegemann, J.P. Glyoxal crosslinking of cell-seeded chitosan/collagen hydrogels for bone regeneration. *Acta Biomater* **7**, 2410, 2011.
42. Chan, B.P., Hui, T.Y., Yeung, C.W., Li, J., Mo, I., and Chan, G.C. Self-assembled collagen-human mesenchymal stem cell microspheres for regenerative medicine. *Biomaterials* **28**, 4652, 2007.
43. Chan, B.P., Hui, T.Y., Wong, M.Y., Yip, K.H., and Chan, G.C. Mesenchymal stem cell-encapsulated collagen microspheres for bone tissue engineering. *Tissue Eng Part C Methods* **16**, 225, 2010.
44. Hui, T.Y., Cheung, K.M., Cheung, W.L., Chan, D., and Chan, B.P. *In vitro* chondrogenic differentiation of human mesenchymal stem cells in collagen microspheres: influence of cell seeding density and collagen concentration. *Biomaterials* **29**, 3201, 2008.
45. Li, C.H., Chik, T.K., Ngan, A.H., Chan, S.C., Shum, D.K., and Chan, B.P. Correlation between compositional and mechanical properties of human mesenchymal stem cell-collagen microspheres during chondrogenic differentiation. *Tissue Eng Part A* **17**, 777, 2011.
46. Cheng, H.W., Luk, K.D., Cheung, K.M., and Chan, B.P. *In vitro* generation of an osteochondral interface from mesenchymal stem cell-collagen microspheres. *Biomaterials* **32**, 1526, 2011.
47. Lennon, D.P., Edmison, J.M., and Caplan, A.I. Cultivation of rat marrow-derived mesenchymal stem cells in reduced oxygen tension: effects on *in vitro* and *in vivo* osteochondrogenesis. *J Cell Physiol* **187**, 345, 2001.
48. Ma, T., Grayson, W.L., Fröhlich, M., and Vunjak-Novakovic, G. Hypoxia and stem cell-based engineering of mesenchymal tissues. *Biotechnol Prog* **25**, 32, 2009.
49. Das, R., Jahr, H., van Osch, G.J., and Farrell, E. The role of hypoxia in bone marrow-derived mesenchymal stem cells: considerations for regenerative medicine approaches. *Tissue Eng Part B Rev* **16**, 159, 2010.
50. Grayson, W.L., Zhao, F., Izadpanah, R., Bunnell, B., and Ma, T. Effects of hypoxia on human mesenchymal stem cell expansion and plasticity in 3D constructs. *J Cell Physiol* **207**, 331, 2006.
51. Buravkova, L.B., and Anokhina, E.B. Effect of hypoxia on stromal precursors from rat bone marrow at the early stage of culturing. *Bull Exp Biol Med* **143**, 411, 2007.
52. Hung, S.P., Ho, J.H., Shih, Y.R., Lo, T., and Lee, O.K. Hypoxia promotes proliferation and osteogenic differentiation potentials of human mesenchymal stem cells. *J Orthop Res* **30**, 260, 2012.
53. Yew, T.L., Huang, T.F., Ma, H.L., Hsu, Y.T., Tsai, C.C., Chiang, C.C., Chen, W.M., and Hung, S.C. Scale-up of MSC

- under hypoxic conditions for allogeneic transplantation and enhancing bony regeneration in a rabbit calvarial defect model. *J Orthop Res* **30**, 1213, 2012.
54. Adesida, A.B., Mulet-Sierra, A., and Jomha, N.M. Hypoxia mediated isolation and expansion enhances the chondrogenic capacity of bone marrow mesenchymal stromal cells. *Stem Cell Res Ther* **3**, 9, 2012.
 55. Ranera, B., Remacha, A.R., Alvarez-Arguedas, S., Castiella, T., Vázquez, F.J., Romero, A., Zaragoza, P., Martín-Burriel, I., and Rodellar, C. Expansion under hypoxic conditions enhances the chondrogenic potential of equine bone marrow-derived mesenchymal stem cells. *Vet J* **195**, 248, 2013.
 56. Owen, M.E., Cavé, J., and Joyner, C.J. Clonal analysis *in vitro* of osteogenic differentiation of marrow CFU-F. *J Cell Sci* **87**, 731, 1987.
 57. Ukai, R., Honmou, O., Harada, K., Houkin, K., Hamada, H., and Kocsis, J.D. Mesenchymal stem cells derived from peripheral blood protects against ischemia. *J Neurotrauma* **24**, 508, 2007.
 58. Horn, P., Bork, S., Diehlmann, A., Walenda, T., Eckstein, V., Ho, A.D., and Wagner, W. Isolation of human mesenchymal stromal cells is more efficient by red blood cell lysis. *Cytotherapy* **10**, 676, 2008.
 59. Horn, P., Bork, S., and Wagner, W. Standardized isolation of human mesenchymal stromal cells with red blood cell lysis. *Methods Mol Biol* **698**, 23, 2011.
 60. Wang, L., Singh, M., Bonewald, L.F., and Detamore, M.S. Signalling strategies for osteogenic differentiation of human umbilical cord mesenchymal stromal cells for 3D bone tissue engineering. *J Tissue Eng Regen Med* **3**, 398, 2009.
 61. Nakamura, A., Dohi, Y., Akahane, M., Ohgushi, H., Nakajima, H., Funaoka, H., and Takakura, Y. Osteocalcin secretion as an early marker of *in vitro* osteogenic differentiation of rat mesenchymal stem cells. *Tissue Eng Part C Methods* **15**, 169, 2009.
 62. Farndale, R.W., Buttle, D.J., and Barrett, A.J. Improved quantitation and discrimination of sulphated glycosaminoglycans by use of dimethylmethylene blue. *Biochim Biophys Acta* **883**, 173, 1986.
 63. Valli, V.E., McGrath, J.P., and Chu, I. Hematopoietic system. In: Haschek, W.M., Rousseaux, C.G., and Wallig, M.A., eds. *Handbook of Toxicologic Pathology*, 2nd edition. San Diego, CA: Academic Press, 2002, pp. 647–679.
 64. Soltan, M., Smiler, D., and Choi, J.H. Bone marrow: orchestrated cells, cytokines, and growth factors for bone regeneration. *Implant Dent* **18**, 132, 2009.
 65. Friedenstein, A.J., Latzinik, N.V., Gorskaya, Yu.F., Luria, E.A., and Moskvina, I.L. Bone marrow stromal colony formation requires stimulation by haemopoietic cells. *Bone Miner* **18**, 199, 1992.
 66. D'Ippolito, G., Schiller, P.C., Ricordi, C., Roos, B.A., and Howard, G.A. Age-related osteogenic potential of mesenchymal stromal stem cells from human vertebral bone marrow. *J Bone Miner Res* **14**, 1115, 1999.
 67. Potier, E., Ferreira, E., Andriamanalijaona, R., Pujol, J.P., Oudina, K., Logeart-Avramoglou, D., and Petite, H. Hypoxia affects mesenchymal stromal cell osteogenic differentiation and angiogenic factor expression. *Bone* **40**, 1078, 2007.
 68. Fehrer, C., Brunauer, R., Laschober, G., Unterluggauer, H., Reitingner, S., Kloss, F., Güllly, C., Gassner, R., and Lepperdinger, G. Reduced oxygen tension attenuates differentiation capacity of human mesenchymal stem cells and prolongs their lifespan. *Aging Cell* **6**, 745, 2007.
 69. Volkmer, E., Kallukalam, B.C., Maertz, J., Otto, S., Drosse, L., Polzer, H., Bocker, W., Stengele, M., Docheva, D., Mutschler, W., and Schieker, M. Hypoxic preconditioning of human mesenchymal stem cells overcomes hypoxia-induced inhibition of osteogenic differentiation. *Tissue Eng Part A* **16**, 153, 2010.
 70. Holzwarth, C., Vaegler, M., Gieseke, F., Pfister, S.M., Handgretinger, R., Kerst, G., and Müller, I. Low physiologic oxygen tensions reduce proliferation and differentiation of human multipotent mesenchymal stromal cells. *BMC Cell Biol* **11**, 11, 2010.
 71. Raheja, L.F., Genetos, D.C., and Yellowley, C.E. The effect of oxygen tension on the long-term osteogenic differentiation and MMP/TIMP expression of human mesenchymal stem cells. *Cells Tissues Organs* **191**, 175, 2010.
 72. Solorio, L.D., Vieregge, E.L., Dhamsi, C.D., and Alsberg, E. High-density cell systems incorporating polymer microspheres as microenvironmental regulators in engineered cartilage tissues. *Tissue Eng Part B Rev* **19**, 209, 2013.
 73. Veronesi, F., Giavaresi, G., Tschon, M., Borsari, V., Nicoli Aldini, N., and Fini, M. Clinical use of bone marrow, bone marrow concentrate, and expanded bone marrow mesenchymal stem cells in cartilage disease. *Stem Cells Dev* **22**, 181, 2013.
 74. Abarrategi, A., López-Morales, Y., Ramos, V., Civantos, A., López-Durán, L., Marco, F., and López-Lacomba, J.L. Chitosan scaffolds for osteochondral tissue regeneration. *J Biomed Mater Res A* **95**, 1132, 2010.
 75. Bhardwaj, N., and Kundu, S.C. Chondrogenic differentiation of rat MSCs on porous scaffolds of silk fibroin/chitosan blends. *Biomaterials* **33**, 2848, 2012.
 76. Majumdar, M.K., Banks, V., Peluso, D.P., and Morris, E.A. Isolation, characterization, and chondrogenic potential of human bone marrow-derived multipotential stromal cells. *J Cell Physiol* **185**, 98, 2000.
 77. Ma, H.L., Hung, S.C., Lin, S.Y., Chen, Y.L., and Lo, W.H. Chondrogenesis of human mesenchymal stem cells encapsulated in alginate beads. *J Biomed Mater Res A* **64**, 273, 2003.
 78. Yang, I.H., Kim, S.H., Kim, Y.H., Sun, H.J., Kim, S.J., and Lee, J.W. Comparison of phenotypic characterization between “alginate bead” and “pellet” culture systems as chondrogenic differentiation models for human mesenchymal stem cells. *Yonsei Med J* **45**, 891, 2004.
 79. Diduch, D.R., Jordan, L.C., Mierisch, C.M., and Balian, G. Marrow stromal cells embedded in alginate for repair of osteochondral defects. *Arthroscopy* **16**, 571, 2000.
 80. Bosnakovski, D., Mizuno, M., Kim, G., Takagi, S., Okumura, M., and Fujinaga, T. Chondrogenic differentiation of bovine bone marrow mesenchymal stem cells (MSCs) in different hydrogels: influence of collagen type II extracellular matrix on MSC chondrogenesis. *Biotechnol Bioeng* **93**, 1152, 2006.
 81. Wu, Y.N., Yang, Z., Hui, J.H., Ouyang, H.W., and Lee, E.H. Cartilaginous ECM component-modification of the microbead culture system for chondrogenic differentiation of mesenchymal stem cells. *Biomaterials* **28**, 4056, 2007.
 82. Ragetly, G., Griffon, D.J., and Chung, Y.S. The effect of type II collagen coating of chitosan fibrous scaffolds on mesenchymal stem cell adhesion and chondrogenesis. *Acta Biomater* **6**, 3988, 2010.
 83. Muschler, G.F., Nakamoto, C., and Griffith, L.G. Engineering principles of clinical cell-based tissue engineering. *J Bone Joint Surg Am* **86-A**, 1541, 2004.
 84. Batorsky, A., Liao, J., Lund, A.W., Plopper, G.E., and Stegemann, J.P. Encapsulation of adult human mesenchymal

- stem cells within collagen-agarose microenvironments. *Biotechnol Bioeng* **92**, 492, 2005.
85. Wang, H., Leeuwenburgh, S.C., Li, Y., and Jansen, J.A. The use of micro- and nanospheres as functional components for bone tissue regeneration. *Tissue Eng Part B Rev* **18**, 24, 2012.
86. Di Martino, A., Sittinger, M., and Risbud, M.V. Chitosan: a versatile biopolymer for orthopaedic tissue-engineering. *Biomaterials* **26**, 5983, 2005.
87. Costa-Pinto, A.R., Reis, R.L., and Neves, N.M. Scaffolds based bone tissue engineering: the role of chitosan. *Tissue Eng Part B Rev* **17**, 331, 2011.

Address correspondence to:

Jan P. Stegemann, PhD

Department of Biomedical Engineering

University of Michigan

1101 Beal Avenue

Ann Arbor, MI 48109

E-mail: jpsteg@umich.edu

Received: March 5, 2013

Accepted: July 17, 2013

Online Publication Date: September 26, 2013

This article has been cited by:

1. Ana Y. Rioja, Ethan L.H. Daley, Julia C. Habif, Andrew J. Putnam, Jan P. Stegemann. 2017. Distributed vasculogenesis from modular agarose-hydroxyapatite-fibrinogen microbeads. *Acta Biomaterialia* **55**, 144-152. [[Crossref](#)]
2. Tongmeng Jiang, Guojie Xu, Qiuyan Wang, Lihui Yang, Li Zheng, Jinmin Zhao, Xingdong Zhang. 2017. In vitro expansion impaired the stemness of early passage mesenchymal stem cells for treatment of cartilage defects. *Cell Death and Disease* **8**:6, e2851. [[Crossref](#)]
3. Joel K. Wise, Andrea I. Alford, Steven A. Goldstein, Jan P. Stegemann. 2016. Synergistic enhancement of ectopic bone formation by supplementation of freshly isolated marrow cells with purified MSC in collagen-chitosan hydrogel microbeads. *Connective Tissue Research* **57**:6, 516-525. [[Crossref](#)]
4. Bornes Troy D., Jomha Nadr M., Mulet-Sierra Aillette, Adesida Adetola B.. 2016. Optimal Seeding Densities for In Vitro Chondrogenesis of Two- and Three-Dimensional-Isolated and -Expanded Bone Marrow-Derived Mesenchymal Stromal Stem Cells Within a Porous Collagen Scaffold. *Tissue Engineering Part C: Methods* **22**:3, 208-220. [[Abstract](#)] [[Full Text HTML](#)] [[Full Text PDF](#)] [[Full Text PDF with Links](#)] [[Supplemental Material](#)]
5. Xie Lili, Mao Mao, Zhou Liang, Jiang Bing. 2016. Spheroid Mesenchymal Stem Cells and Mesenchymal Stem Cell-Derived Microvesicles: Two Potential Therapeutic Strategies. *Stem Cells and Development* **25**:3, 203-213. [[Abstract](#)] [[Full Text HTML](#)] [[Full Text PDF](#)] [[Full Text PDF with Links](#)]
6. Ramkumar Tiruvannamalai Annamalai, David R. Mertz, Ethan L.H. Daley, Jan P. Stegemann. 2016. Collagen Type II enhances chondrogenic differentiation in agarose-based modular microtissues. *Cytotherapy* **18**:2, 263-277. [[Crossref](#)]
7. Xanthippi Chatzistavrou, Rameshwar R. Rao, David J. Caldwell, Alexis W. Peterson, Blake McAlpin, Yuan-Yuan Wang, Li Zheng, J. Christopher Fenno, Jan P. Stegemann, Petros Papagerakis. 2016. Collagen/fibrin microbeads as a delivery system for Ag-doped bioactive glass and DPSCs for potential applications in dentistry. *Journal of Non-Crystalline Solids* **432**, 143-149. [[Crossref](#)]
8. Phuc Van Pham, Ngoc Bich Vu. Production of Clinical-Grade Mesenchymal Stem Cells 107-129. [[Crossref](#)]
9. Ana Y. Rioja, Ramkumar Tiruvannamalai Annamalai, Spencer Paris, Andrew J. Putnam, Jan P. Stegemann. 2016. Endothelial sprouting and network formation in collagen- and fibrin-based modular microbeads. *Acta Biomaterialia* **29**, 33-41. [[Crossref](#)]
10. Xiao Ouyang, Bo Wei, Fengyong Mao, Xiang Zhang, Yan Xu, Liming Wang. 2015. Uncultured bone marrow mononuclear cells delay the dedifferentiation of unexpanded chondrocytes in pellet culture. *Cell and Tissue Research* **361**:3, 811-821. [[Crossref](#)]
11. Emmet M. Thompson, Amos Matsiko, Eric Farrell, Daniel J. Kelly, Fergal J. O'Brien. 2015. Recapitulating endochondral ossification: a promising route to in vivo bone regeneration. *Journal of Tissue Engineering and Regenerative Medicine* **9**:8, 889-902. [[Crossref](#)]
12. Bo Wei, Qingqiang Yao, Yang Guo, Fengyong Mao, Shuai Liu, Yan Xu, Liming Wang. 2015. Three-dimensional polycaprolactone-hydroxyapatite scaffolds combined with bone marrow cells for cartilage tissue engineering. *Journal of Biomaterials Applications* **30**:2, 160-170. [[Crossref](#)]
13. Danielle L. Taylor, Joel J. Thevarajah, Diksha K. Narayan, Patricia Murphy, Melissa M. Mangala, Seakcheng Lim, Richard Wuhler, Catherine Lefay, Michael D. O'Connor, Marianne Gaborieau, Patrice Castignolles. 2015. Real-time monitoring of peptide grafting onto chitosan films using capillary electrophoresis. *Analytical and Bioanalytical Chemistry* **407**:9, 2543-2555. [[Crossref](#)]
14. Ethan L. H. Daley, Rhima M. Coleman, Jan P. Stegemann. 2015. Biomimetic microbeads containing a chondroitin sulfate/chitosan polyelectrolyte complex for cell-based cartilage therapy. *Journal of Materials Chemistry B* **3**:40, 7920-7929. [[Crossref](#)]
15. Sheeny K. Lan Levengood, Miqin Zhang. 2014. Chitosan-based scaffolds for bone tissue engineering. *Journal of Materials Chemistry B* **2**:21, 3161. [[Crossref](#)]
16. A. W. Peterson, D. J. Caldwell, A. Y. Rioja, R. R. Rao, A. J. Putnam, J. P. Stegemann. 2014. Vasculogenesis and angiogenesis in modular collagen/fibrin microtissues. *Biomater. Sci.* **2**:10, 1497-1508. [[Crossref](#)]